Received: 19 October 2017 | Revised: 9 July 2018 | Accepted: 10 July 2018

DOI: 10.1002/adv.22116

RESEARCH ARTICLE

WILEY

Effect of filler content, size, aspect ratio and morphology on thermal, morphological and permeability properties of porous talc filled—Polypropylene obtained through MEAUS process

Kian Habibi | **Pilar Castejón** | **Antonio B. Martínez** | **David Arencón**

Centre Català del Plàstic, Universitat Politècnica de Catalunya, Terrassa, Spain

Correspondence
David Arencón, Centre Català del Plàstic, Universitat Politècnica de Catalunya, C/ Colom 114, E-08222 Terrassa, Spain.
Email: david.arencon@upc.edu

Abstract

Several commercial grades of talc were selected to develop polypropylene based microporous membranes through MEAUS process (melt extrusion—annealing—uniaxial strain). Talc commercial grades differed in particle size, aspect ratio, and crystalline morphology. Different filler percentages were added to polypropylene (1, 5, 10 wt.%) Parameters such as draw ratio during extrusion, annealing temperature strain rate, and strain extension were kept as constant to analyze the effect of the talc characteristics and content of the obtained membranes. Small particle size and high aspect ratio tend to provide membranes with small pore size, high porous area, and high Gurley permeability values.

KEYWORDS

membranes, polypropylene, talc morphology, talc size

1 | INTRODUCTION

Membranes have gained an important place in chemical technology and are used in a broad range of applications. The most important property of membranes is their ability to control the rate of permeation of different species. The key property that is exploited is the ability of a membrane to control the permeation rate of a chemical species through the membrane. A vast number of investigations have so far been carried out on microporous separators as key materials of separation technology. From energy and process reliability points of view, they progressively compete for the conventional separation process such as distillation.[1]

Polymeric membranes are made through various techniques such as phase separation, track etching, leaching, thermal precipitation, and stretching.[1–5] Phase separation is the most employed technology to produce polymeric membranes. Nevertheless, environmental concerns have to be taken into account, such as solvent contamination and costly solvent recovery, although some improvements have been made in the recent decade.

In this study, we have employed a technology based on polymer stretching, called MEAUS (melt extrusion—annealing—uniaxial strain). This procedure is applicable to semicrystalline polymers, based on (a) the stretching of a thin film with a row nucleated lamellar structure (b) annealing of the film to thicken the lamellae, and (c) stretching of the film at low temperature to create voids and then stretching at high temperature to enlarge the pores. One of the main issues in this process is the generation of a proper initial row nucleated structure. The polymer type and applied extrusion conditions are key factors for this method.

The extrusion and production of the precursor films is a delicate process as the samples should be produced under high draw ratio and cooling rates. Obtaining a very uniform film is a major concern as any nonuniformity and thickness variations cause irregularities in the stress distribution. Also, another way to overcome is to enhance the distribution of pores along the membrane face. This method is relatively less expensive and there is no solvent contamination.

Several works are found in the literature, mainly the ones performed by the research group of Ajji,[6] Caihong et al.,[7] focused mainly on the use of neat polyolefins. However,

only a few works deals with filled polyolefin. Nakamura and Nago,[8,9] created the pores through debonding of $CaCO_3$ from the polymeric matrix and also evaluated the dependency of properties of the microporous polypropylene sheets on stretching degree.

Saffar et al.[10] developed polypropylene microporous hydrophilic membranes and changes in the crystalline structure and membrane performance were investigated in details to optimize annealing and stretching conditions. The use of mineral fillers can provide to the membrane an increase in rigidness, an enhancement of the hydrophilic surface characteristic and also can affect to the final porous morphology of the membranes, as most of the fillers have some nucleating ability in the crystallization processes of polyolefins.[7–12]

Caihong et al.[13] used magnesium sulfate whiskers as filler and showed that with increasing whiskers content the porosity of the stretched microporous membranes decreased, whereas the Gurley value showed an increase in values, they also showed that the introduction of $MgSO_4$ up to 10 wt.% did not induce pronounced changes in the pore structure and air permeability properties of the stretched microporous membranes.

Cai et al.[14] indicated that the addition of silicon dioxide into polypropylene microporous membrane leads to the improvement of the mean pore diameter of the stretched microporous membrane, also they showed that the crystalline orientation degree of precursor film decreased, and the Gurley value (characterizing the air permeability) decreased.

In the oil industry, water/oil and gas/oil separation are very crucial, and for this aim, there are three different stages including well-head separation by separators. In the drilling industry, membrane are also employed as a separator in a drilling mud section, where the returning mud from well during the drilling becomes clean of the redundant parts. In the separation of CO_2 from various gas streams, particularly flue gas or stack gas from burning flares, and in case of separation of harmful gases, in refineries, membranes are used as a filter for filtering the outflow gas from flares.[15]

In such cases, mostly calcium carbonate membrane is employed as a separator because of its characteristics and compatibility to catch outflow SO_2 toxic gas from flares to prevent the spreading of SO_2 to the environment and reduce the environmental damages. A $CaCO_3$ membrane gas absorption process is a worthwhile alternative, especially for oil industry plant flue gases by combining the advantages of absorption (high selectivity) and membranes (modularity, small size).[16]

Talc, along with calcium carbonate, is one of the most employed fillers in the plastic industry, so it offers an interesting alternative in the development of membranes used in oil separator industry. Talc has a well-known nucleating activity on the crystallization of polypropylene[17,18] and hydrophilicity.

Talc, $Mg_3Si_40_{10}(OH)_2$ is a trioctahedral phyllosilicate, macroscopically hydrophobic as it floats naturally with no layer charge.[19,20] However, upon outgassing, controlled rate thermal analysis measurements coupled with mass spectrometric analyzes show that different surface species (water, nitrogen, carbon dioxide, and organic molecules) are released from the talc surface.[19]

On outgassed talc, the adsorption of water seems to occur through the growth of hydrogen-bonded clusters anchored on the hydroxyl group controlled by the presence of highly hydrophilic sites isolated on a hydrophobic surface. Talc then behaves as a specific material as very strong interaction occurs between the hydroxyl group and polarizable molecules. The hydroxyl group of the octahedral layer mainly controls the surface behavior of talc, which points directly toward the basal surfaces, because of the perfect trioctahedral nature of the mineral. In the natural state, organic and inorganic species are adsorbed on the talc surface and screen these highly energetic sites, so it should be expected a water absorption in such kind of water-oil separator systems.[20]

No works are found in the literature concerning the use of talc in microporous membranes obtained by extrusion. An increase in the orientation of precursor films could consider as one of the possible results. We also hypothesize that the addition of talc to polypropylene could affect the special kind of crystallization (row lamellar) that a polypropylene develops in MEAUS process, and subsequently would affect the pore morphology.

This work is the first stage of this study, in where the key point is the combination of an advanced modification of the extrusion process (rapid air cooling) of the extruded exit along with the addition of talc of mineral filler. In this study, several types of talc, differing in particle size, morphology and aspect ratio will be added at different concentration polypropylene, to analyze the effect of these characteristics on physical and transport properties of membranes produced through MEAUS process.

2 | MATERIALS

A commercial extrusion grade with tradename PP020 kindly supplied by *Repsol S.A.* has been selected. The melt flow rate (230°C, 2.16 kg) was 1.0 dg/min. Average number and mass molecular weights were $M_n = 119$ kg/mol and $M_W = 659$ kg/mol respectively, showing a monomodal mass molecular weight distribution. Five different commercial talc grades differing in particle size, morphology, and specific surface area were kindly supplied by *Imerys Talc*. Micrographs accounting for talc morphology are depicted in Figure 1.

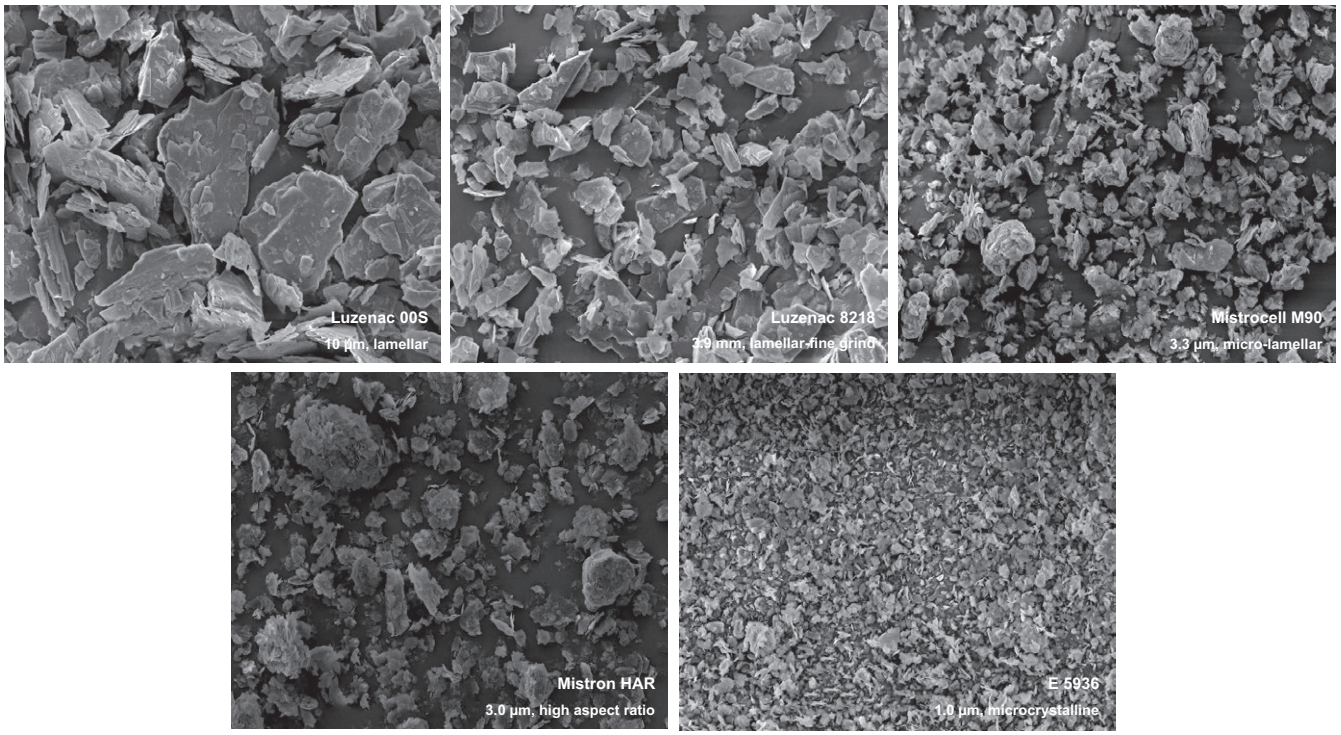

FIGURE 1 SEM micrographs of particle average size and morphology of the employed talc grades. Magnification ×1,000, 10 µm

3 | EXPERIMENTAL PROCEDURE

3.1 | Film extrusion and membrane preparation

Polypropylene-talc films (1, 5, 10 wt.% talc) were prepared by melt mixing using co-rotating twin screw extruder (length/diameter = 36, diameter = 25 mm) at a constant rotating speed of 40 rpm and a die temperature of 240°C. At the end of the extruder, a rectangular cross-section die was adapted, with nominal dimensions 122 × 1.9 mm. At these processing conditions, output pressure was high enough and constant to allow the extrudate to come out from the extrusion die. A system of two air knives was mounted close to the die to provide air to the outgoing film surface right at the exit of the die and get a fast cooling. Cooling air pressure was kept to 15 bar. After the air knife, a three-cylinder system pulled the cooled film at the constant speed of rotation, kept the outgoing film in a constant stretching condition, and provided a nominal draw ratio of 70 (Figure 2). The nominal thickness of the films ranged between 25 and 35 µm.

All the extruded films were annealed at 140°C for 15 min in an oven. For final membrane fabrication, rectangular samples with nominal dimensions 75 × 60 mm were cut out from the annealed films. The uniaxial strain on these rectangular samples was performed in a universal testing machine *Galdabini Sun 2500*, dotted with a load cell of 1 kN and a climatic chamber. The uniaxial strain was carried out in two stages: cold stage: 23°C, using a crosshead speed of 50 mm/min, reaching an elongation of 35%; hot stage: 140°C, using a crosshead speed of 10 mm/min reaching a total elongation of 200%.

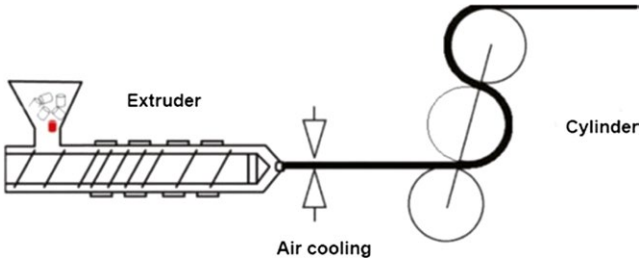

FIGURE 2 Summary outline of the precursor film manufacturing process

3.2 | Polarized Fourier Transform Infrared spectroscopy

Infrared spectra were obtained using a spectrophotometer *FT-IR Perkin Elmer Spectrum 1000* (resolution 1 cm^{-1}), equipped with a light polarizer. The absorbance determined with polarized light at 0º is parallel ($A\|\|$) to the extrusion flow of the precursor film. By other hand, the absorbance determined with a polarized light at 90º is perpendicular ($A\perp$) to the extrusion flow. With these values, the dichroic relationship (D) could be obtained:

$$D = \frac{A||}{A\perp} \quad (1)$$

For PP, the crystalline phase orientation (F_c) is obtained from the values of absorbance of the band at 998 cm^{-1}, measured at 0° and 90°, from Herman expression.[21]

$$F_c = \frac{D-1}{D+2} \quad (2)$$

3.3 | Thermal analysis

Crystallization behavior of the obtained membranes was analyzed using a *TA Instruments Q1000* differential scanning calorimeter. A heating cycle from 30 to 200°C at 20°C/min was performed on the membranes. For comparison purposes, pellets of the different compounds were kept for 3 min at 200°C, cooled to 30°C at 20°C/min and finally heated from 30 to 200°C at 20°C/min. The alleged crystallinity results were obtained using a heat of fusion of 207.1 J/g for theoretically fully crystalline polypropylene.[22]

3.4 | Morphology

Scanning electron microscopy was employed (*JEOL JSM-5610*) for the analysis of the membrane pore structure. The membranes were previously gold-coated to ascertain electrical conductivity. The micrographs were analyzed through the software *Buehler Omnimet*. Values of pore size, and porous surface area were obtained. For calculation, a circular-like porous geometry was assumed.

3.5 | Permeability

The permeability of membrane toward air was measured by Gurley equipment. It was determined the time for a settled volume (50 ml) of air to pass through the membrane with a fixed area (0.79 cm^2) under the pressure of 0.02 MPa. In general, high Gurley value corresponds to low air permeability and a long tortuous path for air transportation, implying higher curvature for pores. A value of permeability was obtained through the following calculation initially by measuring the correction factor, and then based on that the main permeability calculation computes:

$$Z = \text{permeability (seconds)}/(4.1461) \quad (3)$$

$$\text{Permeability}, \mu\text{m}/\text{Pa s} = 135.5/z \quad (4)$$

where Equation (3), Z represents the correction factor measurement based on Gurley equipment manual for obtained data from Gurley machine and then followed by Equation (4) in whereby substituting the obtained Z from the previous equation in the Equation (4) the main calculation of Permeability computes.

4 | RESULTS AND DISCUSSION

4.1 | The orientation of precursor films

Several works account for the needing of a highly oriented row lamellar structure in neat polypropylene films, so as membranes could be obtained in next stages of MEAUS processes; the minimum orientation factor should be above 0.35.[21,23] In the precursor films, the orientation and position of the crystal blocks control the lamellae separation process, which leads to pores formation. The orientation of the crystalline phase of the precursor films has been measured by Fourier-transform infrared spectroscopy.

Orientation factors of our study are showed in Table 1. The addition of talc constraint the orientation of neat polypropylene, being this effect more marked as more amount of talc is added to polypropylene. This observation is different of that observed for injection molding of talc-based composites, in which the concomitance of orientation of the chains and the talc platelets is a common feature observed in other processes as for example injection molding,[24,25] tending to align along the flow direction, enhanced by the so-called shear-amplification effect. Small shear effects in MEAUS process rather than in injection molding could explain the reduction in the global orientation of the precursor films when talc is added. Small differences are observed referring to the morphology, particle size and BET area of talc. Nevertheless, it seems that high aspect ratio talc (more oriented) combined with small particle size and high BET area helps to minimize the descent of orientation factors when higher amounts of talc are added. Probably the increase in talc content leads to some agglomeration of particles, then create a more spherical-like morphology, that is against a preferential orientation of the polymer when it comes out from the extrusion die. Holland et al.[26] showed that at higher (aspect ratio) a platy (upper) boundary is reached and at this boundary, the morphology is essentially a constant and the particle size alone determines the surface area. As talc becomes less platy, the particles form increasingly foliated aggregates.

The surface area of talc cannot be directly related to its particle size although the particle size is directly related to the talc morphology and is inversely related to the specific surface area. Hence, talc particles with high aspect ratio filler and also talc particles with micro-lamellar morphology probably are orientated in the PP matrix. Morphological observations by SEM (Figure 1) show that talc samples with higher particle sizes and lower surface areas are constituted by very fine flakes, without arrangement, characteristic of lamellar and micro-lamellar, while talc samples with smaller in particle sizes and higher in surface areas present high aspect ratio and microcrystalline with long, well stacked-up flakes.

TABLE 1 Properties and permeability of the microporous membranes prepared using Gurley equipment

Reference	Morphology	Particle size	BET (m^2/g)	Talc content (wt.%)	F_c	Average porous size (μm)	Percentage of porous area	Gurley permeability 10^3 μm/Pa s
Neat PP	—	—	—	0	0.61	0.15	16.0	110
L 00S	Lamellar	10.0	2.4	1	0.49	0.07	5.0	120
				5	0.26	0.07	5.2	101
				10	0.24	0.07	4.8	100
L 8218	Lamellar—fine grind	3.9	5.4	1	0.52	0.06	14.5	109
				5	0.29	0.07	12.1	100
				10	0.26	0.06	12.8	71
M 90	Micro-lamellar	3.3	13.0	1	0.56	0.07	13.6	138
				5	0.33	0.07	15.9	124
				10	0.29	0.06	12.5	100
M HAR	High aspect ratio	3.0	13.0	1	0.52	0.06	16.2	132
				5	0.35	0.05	16.2	117
				10	0.35	0.07	15.0	103
E 5936	Microcrystalline	1.1	21.3	1	0.45	0.07	15.6	116
				5	0.30	0.06	8.6	110
				10	0.26	0.06	7.3	104

4.2 | Differential scanning calorimetry analysis

Results from DSC analysis are summarized in Table 2. It is well established in the literature, the nucleation ability that talc has onto the crystallization process of polypropylene.[19,26] Cooling runs carried out on sample pellets displays that talc rises the crystallization peak temperature up to 5°C with respect of neat polypropylene, by just adding 1 wt.% of talc; this effect is even more marked as the talc content is increased (Figure 3a). This nucleation effect is lower than in other works related to this topic; it seems that the high molecular weight polypropylene employed in this work (extrusion grade) restricts the high ability of talc to shift the crystallization onset to higher temperatures. Perego et al.[27] described that at equal conditions, due to an increase in chain mobility, lower molecular weights have more time to complete crystallization. When talc is present in polypropylene, we suggest that during crystallization only a few polypropylene chains can align themselves on talc surface, thus causing the apparition of a nucleus site on the mineral surface. The substrate can influence crystallites growth into a particular orientation, in which, together with a nuclear density increase, will shorten the duration of the crystallization process.

Small differences can be observed, above all at high filler contents, when using talc with small particle size—high BET area, what could be related to the highest available surface area of talc to interact with polypropylene matrix related with the talc nature, talc size, and talc BET area. This could be related with the ability of promoting crystalline nuclei. Global crystallization at cooling run conditions showed a reduction in the crystallinity values with respect of neat PP. Being more marked as talc content is increased, as high loads, the filler particles generate a physical barrier to the crystal lamella growth and thus limit the global crystallization efficiency. Despite the fact that talc is a good nucleating agent for polypropylene, in this study, we surprisingly can see the reduction in crystallization temperature. The inclusion of talc with small particles into polypropylene might have caused reducing in crystallization temperature and might cause this effect which talc particles may induce heterogeneous nucleation during crystallization and considerably reduced the crystallization of PP/talc as we can see in Table 2 or morphologically, talc might have reduced the spherulite dimension of the PP/talc during crystallization. Although talc particles increased the crystallization temperature compared with that of neat polypropylene.

DSC tests performed on membranes outstands the strong influence of the actual crystallization process that is taking place when producing membrane film precursors through extrusion. Figure 3b,c display the different shape of melting peaks between precursor films. A bimodal distribution is found in membranes. First of all, the interval of temperatures at which melting of membranes takes places is generally broader than the one from precursor films melting. Second, a shoulder attached to the main melting

TABLE 2 Results obtained from thermal analysis from DSC

					Cooling runs		Heating runs				
Ref.	**Morphology**	**Particle size**	**BET (m^2/g)**	**Talc (wt.%)**	**P-X_c (%)**	**P_c-Peak**	**PF-X_m (%)**	**PF_m Peak**	**M-X_m (%)**	**M Peak (°C)**	**2_{nd} M-M-Peak (°C)**
Neat PP	—	—	—	0	50.8	114.0	48.1	162	48.3	163.7	172.7
L 00S	Lamellar	10.0	2.4	1	44.9	119.7	44.5	162.2	51.0	165.7	176
				5	41.5	121.6	41.0	162.9	51.9	166.3	179.2
				10	39.2	122.9	38.8	162.7	42.9	165.5	174.2
L 8218	Lamellar—fine grind	3.9	5.4	1	44.4	119.5	43.8	163.2	53.5	164.9	178
				5	38.8	120.7	37.8	164.2	51.4	165.5	175.4
				10	38.7	122.2	38.7	163.8	36.5	165.6	172.4
M 90	Micro-lamellar	3.3	13.0	1	41.5	119.1	40.0	163.8	48.9	165.1	174.7
				5	40.4	122.5	40.8	163.5	47.8	163.8	174.8
				10	39.2	123.8	38.1	163.9	45.9	165.8	174.1
M HAR	High aspect ratio	3.0	13.0	1	45.5	120.1	44.3	162.5	51.1	164.9	176.7
				5	43.8	121.1	42.4	163.9	45.6	164.7	176.4
				10	39.5	124.5	38.1	164.2	40.3	165.6	174.4
E 5936	Microcrystalline	1.1	21.3	1	41.6	120.1	40.3	164.3	49.9	164.9	175.1
				5	41.4	122.5	40.1	164.1	45.1	165.4	175.5
				10	37.1	124.5	37.4	164.2	38.9	165.3	176.2

Note. Acronyms for cooling runs P-X_c (pellet crystallinity); P_c-Peak (pellet crystallization peak); Acronyms for heating runs PF-X_m (precursor film melting crystallinity); PF_m Peak (precursor film melting peak); M-X_m (membrane melting crystallinity); M-Peak (membrane melting peak); M-2_{nd} peak (membrane second melting peak).

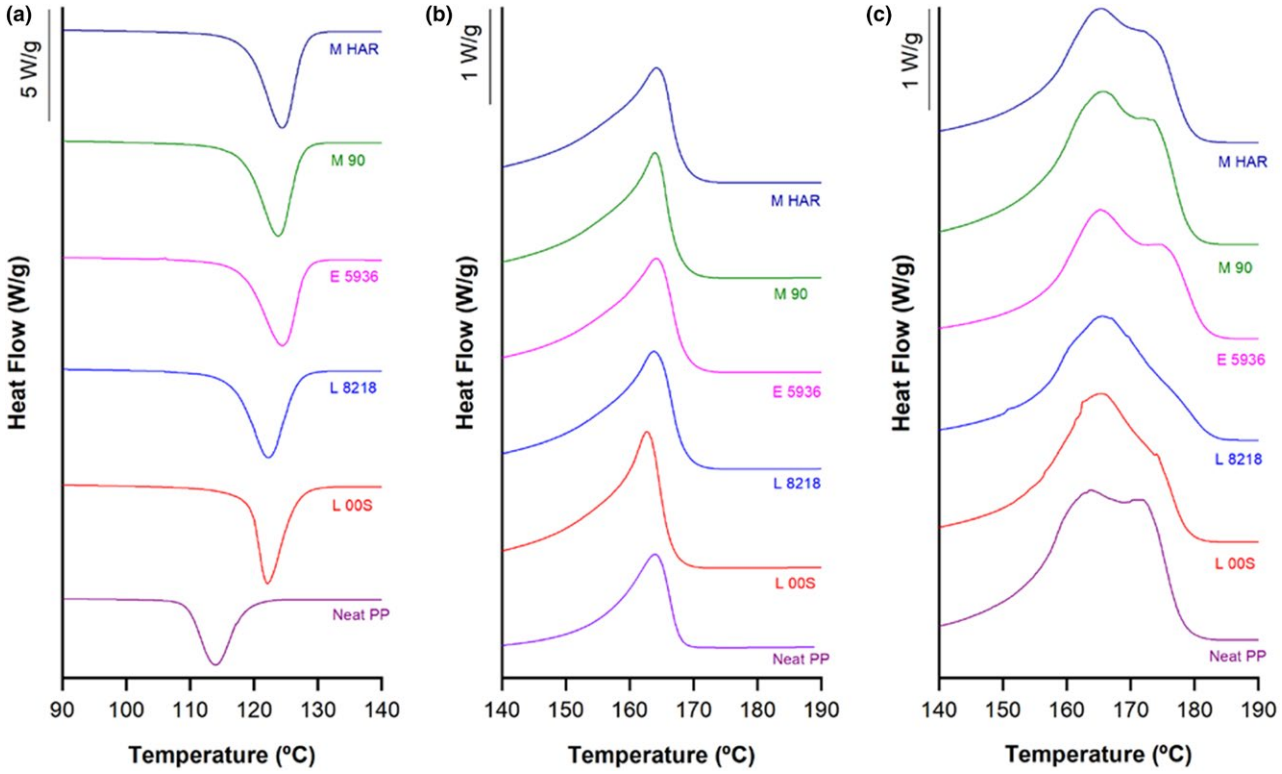

FIGURE 3 DSC thermograms obtained from neat PP and 10 wt.% talc compounds on (a) pellets (cooling runs); (b) precursor films and (c) membranes (heating runs)

peak appears in membranes. Several works allocate this phenomenon to[23,27] the melting of a secondary crystalline fraction of lesser stability and size, formed during slow isothermal crystallization (annealing stage). This slow crystallization was carried out when annealing the precursor films at 140°C for 15 min previous to the drawing and production of membranes. It is surprising that the secondary peaks of the talc-based membranes appear at higher temperatures, indicating that talc has promoted more stable and greater crystalline entities during annealing. As we have employed a homopolymer grade of polypropylene the shoulder peak can only be attributed to lamellae distribution (thinner and thicker lamellae). It is assumed that one of these peaks corresponds to crystals of the interconnected bridges between the lamellae and the other reflects the lamellae crystals.[28–30]

Seguela et al.[31] they reported the transition of metastable phase to more stable a-PP crystals during deformation process. They also showed that this endotherm revealed a smectic metastable phase, which was produced when a polypropylene film was extruded and rapidly cooled to room temperature. The smectic phase could transform into monoclinic α-form when annealed at temperatures above 60°C.

Dudic et al.[32] illustrated that there was no direct relationship between the endotherm peak and smectic phase. They attributed the existence to the crystallization of polymer portions which were somewhere between amorphous and smectic phases.

Primary melting peak shifts to higher temperatures in membranes with respect to precursor films. Talc addition tends to increase this trend. Small differences between the different types of talc are observed, with regard of the primary melting peak of membranes, but in secondary melting peak, there are differences concerning to the width of the secondary melting peak, being broader when using microcrystalline talc.

The appearance of the secondary melting peak has as a consequence an increase in the crystallinity values obtained from melting signals when comparing membrane signals to precursor films signals. Even more interesting is the fact that in pellets run, talc, hinders crystallization, but in membrane runs, talc enhances crystallization. This is another evidence of the key role of talc during the crystallization under strong straining and cooling conditions.

4.3 | Morphology of membranes and permeability

Table 1 obtained from image analysis of SEM morphology (Figures 4 and 5) the numerical analysis related to membrane morphology and Gurley permeability, pore size of neat polypropylene is approximately twice greater in size than talc/

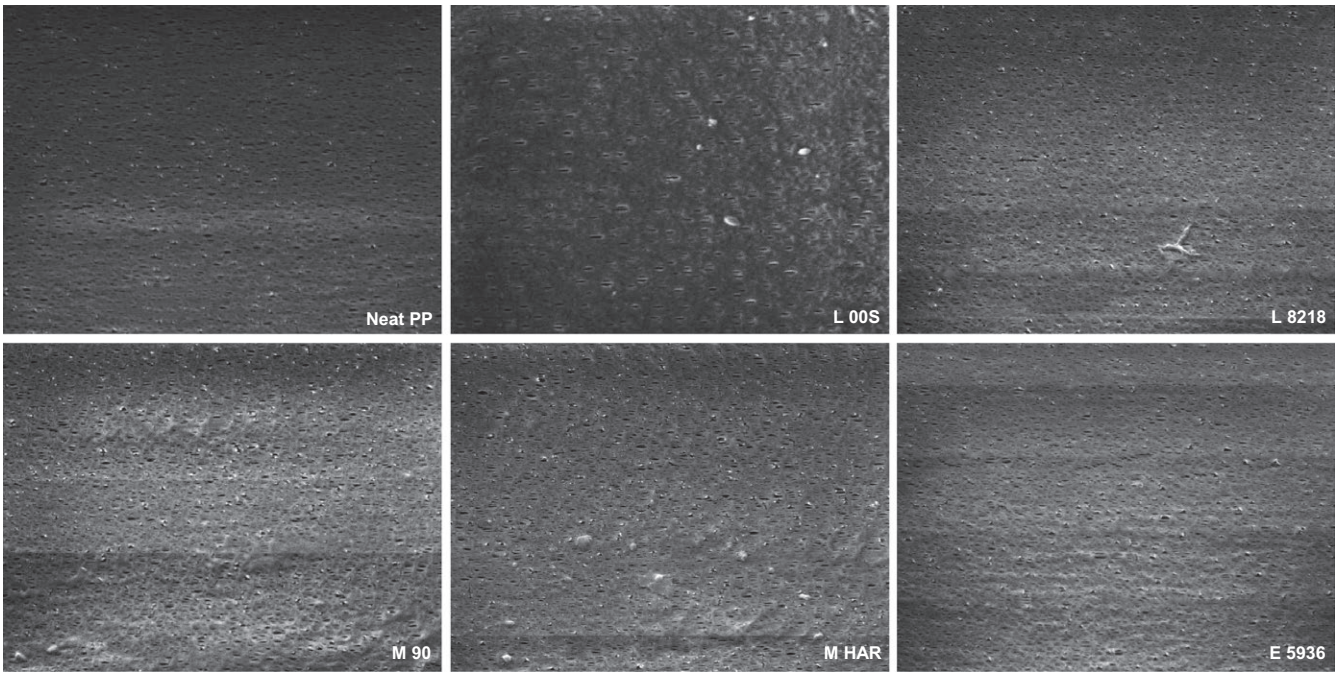

FIGURE 4 Surface morphologies of membranes of neat PP and talc-based membranes with 1 wt.% talc

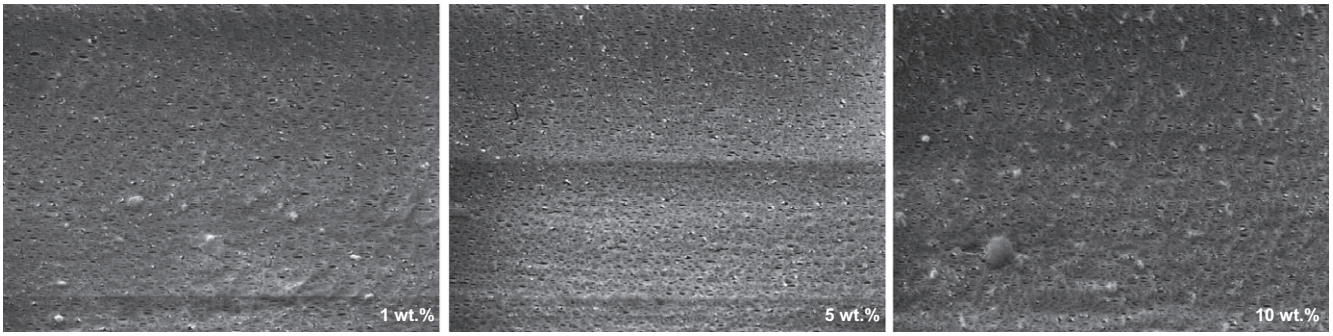

FIGURE 5 Surface morphologies of M HAR-based membranes with different talc contents

based membranes. In this sense, talc might constrain the growth of nucleated pore during cold strain stage during the drawing of the precursor films, just for the physical barrier of inorganic particles dispersed in a polypropylene matrix. Also, it can be observed that pore distribution along the membrane surface is much more homogeneous in talc-based membranes rather than in neat polypropylene membrane, in which there are some zones with no pores.

Nevertheless, despite the bigger pore size, the total area of membrane covered by pore is much less extensive in neat polypropylene. The strong nucleation activity of talc particles seems to help the nucleation of the pore, and also, some micro debonding around talc particles during drawing may be taking place, giving, as a result, a much more porous surface in talc-based membranes.

Talc size has an enormous influence on the generation of a more porous surface. It can be seen that bigger particle size results in the lower porous area. These lower particle surface areas provide less interaction with polypropylene matrix and thus, the micro debonding area is less extensive. The explanation of the low porosity area in very fine particles, above all when high amounts of talc are added, can be based on agglomeration effects, resulting in a reduction in the potential surface area of the talc to interact with polypropylene matrix.

The key role of an enhanced interaction between talc and polypropylene stands out when analyzing the geometry of talc. It is observed that the highest talc BET area (micro-lamellar and high aspect ratio grades) is beneficial in terms of increasing porous area. Microcrystalline takes advantage also of this strong interaction, but only with small amounts of talc; the negative effect of agglomeration prevails against BET area when high amounts of talc are employed. Lowest BET area gives the lowest values of porosity area.

Permeability values reveal that not only porous area is the key factor that determines the global permeability, but the tortuosity and pore geometry along the thickness of the membranes is of importance. This is evidenced by the fact similar values of porous area (e.g., neat PP and M HAR-talc-based membranes have similar values of porous surface area, but the global permeability is higher in talc-based membranes). According to the results of porous area, there is a pretty logical relationship between the percentage of porous area and permeability values. Highest permeability Gurley values are achieved when high aspect ratio, medium size, and low content of talc is employed.

5 | CONCLUSIONS

Differences in orientation, thermal behavior, pore morphology, and permeability are observed with the addition of talc particles in the PP matrix, referring to the morphology, particle size, and BET area of talc. High aspect ratio talc (more oriented) combined with small particle size and high BET area helps to minimize the descent of orientation factors when higher amounts of talc are added. Tests carried on membranes outstands the strong influence of the actual crystallization process that is taking place when producing membrane film precursors through extrusion. Cooling runs performed on sample pellets shows that talc rises the crystallization peak temperature up to 5°C with respect of neat polypropylene, by adding 1 wt.% of talc; this effect is even more marked as the talc content is increased. A bimodal distribution was found in melting peak of membranes. Talc addition shifted to higher temperatures the shoulder of membrane melting peak. Morphology of the produced membranes and analysis of numerical data related to membranes and Gurley permeability elucidated Pore size of neat polypropylene is approximately twice greater in size than talc/based membranes, also it can be observed in pore distribution along the membrane surface is much more homogeneous in talc-based membranes rather than in neat polypropylene membrane, in which there are some zones with no pores. Permeability values show that not only porous area is the key factor that determines the global permeability but also according to the results of the porous area, there is a logical relationship between the percentage of the porous area and permeability values.

ACKNOWLEDGMENTS

The authors would like to acknowledge the Ministerio de Economía, Industria y Competitividad (Government of Spain) for the financial support of project MAT2017-89787-P.

ORCID

David Arencón http://orcid.org/0000-0002-9517-0891

REFERENCES

[1] R. W. Baker, Membrane Technology and Applications, Wiley, Chichester, UK **2004**.
[2] F. Sadeghi, A. Ajji, P. J. Carreau, *J. Membr. Sci.* **2007**, *292*, 62.
[3] F. Sadeghi, A. Ajji, P. J. Carreau, *J. Polym. Sci. B Polym. Phys.* **2008**, *46*, 148.
[4] S. H. Tabatabaei, Development of microporous membranes from PP/HDPE films through cast extrusion and stretching **2009**, *345*, 148.
[5] S. H. Tabatabaei, P. J. Carreau, A. Ajji, *J. Membr. Sci.* **2008**, *325*, 772.
[6] F. Sadeghi, A. Ajji, P. J. Carreau, *Polym. Eng. Sci.* **2007**, *47*, 1170.
[7] L. Caihong, H. Weiliang, X. Ruijie, X. Yunqi, *J. Plast. Film Sheet.* **2012**, *28*, 151.
[8] S. Nakamura, S. Kaneko, Y. Mizutani, *J. Appl. Polym. Sci.* **1993**, *49*, 143.
[9] S. Nagō, Y. Mizutani, *J. Appl. Polym. Sci.* **1998**, *68*, 1543.
[10] A. Saffar, P. J. Carreau, A. Ajji, M. R. Kamal, *J. Membr. Sci.* **2014**, *462*, 50.
[11] A. Qaiss, H. Saidi, O. Fassi-Fehri, M. Bousmina, *J. Appl. Polym. Sci.* **2012**, *123*, 3425.
[12] J. Zhang, J. Fang, J. L. Wu, J. Wu, H. Mo, Z. M. Ma, N. L. Zhou, J. Shen, *Polym. Compos.* **2011**, *32*, 1026.
[13] L. Caihong, Q. Cai, R. Xu, X. Chen, J. Xie, *J. Appl. Polym. Sci.* **2016**, *133*, 43884.
[14] Q. Cai, R. Xu, X. Chen, C. Chen, H. Mo, C. Lei, *Polym. Compos.* **2016**, *37*, 2684.
[15] T. Hirata, H. Nagayasu, T. Yonekawa, M. Inui, T. Kamijo, Y. Kubota, T. Tsujiuchi, D. Shimada, T. Wall, J. Thomas, *Energy Procedia* **2014**, *63*, 6120.
[16] M. Rezakazemi, M. Sadrzadeh, T. Matsuura, *Prog. Energy Combust. Sci.* **2018**, *66*, 1.
[17] J. Velasco, J. De Saja, A. Martinez, *J. Appl. Polym. Sci.* **1996**, *61*, 125.
[18] M. Xanthos, C. Chandavasu, K. Sirkar, C. Gogos, *Polym. Eng. Sci.* **2002**, *42*, 810.
[19] L. J. Michot, F. Villieras, M. Francois, J. Yvon, R. Le Dred, J. M. Cases, *Langmuir* **1994**, *10*, 3765.
[20] B. Rotenberg, A. J. Patel, D. Chandler, *J. Am. Chem. Soc.* **2011**, *133*, 20521.
[21] S. H. Tabatabaei, P. J. Carreau, A. Ajji, *Polymer* **2009**, *50*, 4228.
[22] K. Ishikiriyama, B. Wunderlich, *J. Polym. Sci. B Polym. Phys.* **1997**, *35*, 1877.
[23] E. Ferrage, F. Martin, S. Petit, S. Pejo-Soucaille, P. Micoud, G. Fourty, J. Ferret, S. Salvi, P. De Parseval, J. Fortune, Evaluation of talc morphology using FTIR and H/D substitution 5 October 2000 **2003**.
[24] M. Alonso, J. Velasco, *Eur. Polym. J.* **1997**, *33*, 255.
[25] S. Guo, *Chinese J. Polym. Sci.* **2015**, *33*, 1028.
[26] H. Holland, M. Murtagh, *Adv. X-ray Anal.* **2000**, *42*, 421.
[27] G. Perego, G. D. Cella, C. Bastioli, *J. Appl. Polym. Sci.* **1996**, *59*, 37.

[28] R. H. Rane, K. Jayaraman, K. L. Nichols, T. R. Bieler, M. H. Mazor, *J. Polym. Sci. B Polym. Phys.* **2014**, *52*, 1528.
[29] F. Qiu, M. Wang, Y. Hao, S. Guo, *Compos. Part A Appl. Sci. Manuf.* **2014**, *58*, 7.
[30] A. Makhlouf, H. Satha, D. Frihi, S. Gherib, R. Seguela, *Express Polym. Lett.* **2016**, *10*, 237.
[31] R. Seguela, E. Staniek, B. Escaig, *J. Appl. Polym. Sci.* **1999**, *71*, 1873.
[32] D. Dudic, D. Kostoski, V. Djokovic, *Polym. Int.* **2002**, *51*(2), 111.

How to cite this article: Habibi K, Castejón P, Martínez AB, Arencón D. Effect of filler content, size, aspect ratio and morphology on thermal, morphological and permeability properties of porous talc filled—Polypropylene obtained through MEAUS process. *Adv Polym Technol*. 2018;37:3315–3324. https://doi.org/10.1002/adv.22116